AD-A075 685 LOCKHEED MISSILES AND SPACE CO INC PALO ALTO CA PALO --ETC F/G 12/1
PARTITIONED TRANSIENT ANALYSIS PROCEDURES FOR COUPLED-FIELD PRO--ETC(U)
JUL 79 K C PARK , C A FELIPPA N00014-74-C-0355
UNCLASSIFIED LMSC/D678072 NL

1 OF 1
AD-
A075685

END
DATE FILMED
11-79
DDC

LEVEL II

(10)

PARTITIONED TRANSIENT ANALYSIS PROCEDURES FOR COUPLED-FIELD PROBLEMS: ACCURACY ANALYSIS

K. C. Park and C. A. Felippa
Applied Mechanics Laboratory
Lockheed Palo Alto Research Laboratory
3251 Hanover Street
Palo Alto, CA 94304

July 1979

UNCLASSIFIED
SECURITY CLASSIFICATION OF THIS PAGE (When Data Entered)

REPORT DOCUMENTATION PAGE

READ INSTRUCTIONS BEFORE COMPLETING FORM

1. REPORT NUMBER: LMSC-D678072	2. GOVT ACCESSION NO.
3. RECIPIENT'S CATALOG NUMBER	
4. TITLE (and Subtitle): PARTITIONED TRANSIENT ANALYSIS PROCEDURES FOR COUPLED-FIELD PROBLEMS: ACCURACY ANALYSIS.	5. TYPE OF REPORT & PERIOD COVERED: Technical Report.
	6. PERFORMING ORG. REPORT NUMBER
7. AUTHOR(s): K. C. Park and C. A. Felippa	8. CONTRACT OR GRANT NUMBER(s): N00014-74-C-0355
9. PERFORMING ORGANIZATION NAME AND ADDRESS: Applied Mechanics Laboratory (52-33/205), LOCKHEED PALO ALTO RESEARCH LABORATORY, 3251 Hanover Street, Palo Alto, CA 94304	10. PROGRAM ELEMENT, PROJECT, TASK AREA & WORK UNIT NUMBERS
11. CONTROLLING OFFICE NAME AND ADDRESS: Office of Naval Research, Department of the Navy, Arlington, VA 22217	12. REPORT DATE: July 1979
	13. NUMBER OF PAGES: 31
14. MONITORING AGENCY NAME & ADDRESS(if different from Controlling Office)	15. SECURITY CLASS. (of this report): UNCLASSIFIED
	15a. DECLASSIFICATION/DOWNGRADING SCHEDULE

16. DISTRIBUTION STATEMENT (of this Report)

Approved for Public Release; Distribution Unlimited.

17. DISTRIBUTION STATEMENT (of the abstract entered in Block 20, if different from Report)

18. SUPPLEMENTARY NOTES

19. KEY WORDS (Continue on reverse side if necessary and identify by block number)

Coupled-field problems, partitioned procedures; implicit-explicit procedures, implicit-implicit procedures, numerical stability, direct time integration technique

20. ABSTRACT (Continue on reverse side if necessary and identify by block number)

Partitioned solution procedures for direct time integration of second-order coupled-field systems are studied from the standpoint of accuracy. Such procedures are derived by three formulation steps: implicit integration of coupled governing equations, algebraic partitioning, and extrapolation to advance the solution. It is shown that the combined effect of partition, extrapolation and computational paths, dictates the choice of stable extrapolators and the preservation of rigid-body motions. Stable extrapolators for various computational paths are derived

(continued)

DD FORM 1 JAN 73 1473 EDITION OF 1 NOV 65 IS OBSOLETE

210118

UNCLASSIFIED
SECURITY CLASSIFICATION OF THIS PAGE (When Data Entered)

Item 20. Abstract (continued)

and implementation-extrapolator combinations which preserve rigid-body motions are identified. A spectral analysis shows that the partition itself, when stable, affects primarily frequency distortion. Finally, the advantages and shortcomings of five partitioned procedures are discussed as a guide to practical applications.

ABSTRACT

Partitioned solution procedures for direct time integration of second-order coupled-field systems are studied from the standpoint of accuracy. Such procedures are derived by three formulation steps: implicit integration of coupled governing equations, algebraic partitioning, and extrapolation to advance the solution. It is shown that the combined effect of partition, extrapolation and computational paths, dictates the choice of stable extrapolators and the preservation of rigid-body motions. Stable extrapolators for various computational paths are derived and implementation-extrapolator combinations which preserve rigid-body motions are identified. A spectral analysis shows that the partition itself, when stable, affects primarily frequency distortion. Finally, the advantages and shortcomings of five partitioned procedures are discussed as a guide to practical applications.

TABLE OF CONTENTS

INTRODUCTION

The computer simulation of coupled-field dynamic systems generally involves two distinct phases. A spatially discretized model is produced through finite element, boundary element or finite difference techniques. The resulting equations of motion are then solved by direct time integration.

Often the response charactertistics of the component (single-field) subsystems are markedly different. As examples of this situation we can cite fluid-structure, soil-structure, and certain structure-structure interaction problems. This difference may be due to material properties, different spatial discretization techniques, localized nonlinearities, boundary layer effects, or other computational considerations.

For coupled systems befitting the preceding description, it is natural to think of tailoring the time integration procedure to subsystem response features. An efficient way of implementing this strategy is to view each single-field subsystem as a computational entity, which is treated by an appropriate time integration program module ("analyzer"). The time-advancing process results from coordinating the execution of the analyzers in sequential or parallel fashion. Field coupling effects are incorporated through cyclic information transfers predicated through appropriate extrapolation formulas. Solution procedures based on this approach were called partitioned transient analysis procedures (or simply partitioned procedures) in [1]. In this paper, a general partitioning procedure was presented for treating second-order coupled-field equations of motion.

The rational selection of a specific partitioning procedure among competing ones demands an understanding of numerical stability and accuracy characteristics. In [1], a general stability analysis technique was developed to eliminate case-by-case stability considerations. This technique has provided a common basis for evaluating procedures on grounds of stability, which is critical in the initial method-design stages.

Once satisfactory stability requirements are achieved, it remains to assess accuracy. The understanding of this subject has so far been based largely on numerical experiments [2-7]. This paper endeavors to fill the void by developing an accuracy assessment theory. More specifically, the following three points are addressed: (a) strong interdependency of accuracy, extrapolator formula, and computational sequence details; (b) preservation of rigid-body motions under partitioning; and (c) incremental effect of partitioning on numerical damping and frequency distortion measures. These three aspects provide sufficient grounds for a comparative assessment of competing stable procedures.

REVIEW OF PARTITIONED PROCEDURES

The three basic formulation steps discussed in [1] are: implicit time discretization of the entire system of coupled field equations; partitioning of the coefficient matrix (herein termed solution matrix) that premultiplies the current state vector; and application of extrapolators to the current-state terms that end up on the right-hand side of the partitioned algebraic equations. The resulting partitioned procedure embodies those previously proposed by Belytschko and Mullen [2,3], Park, Felippa and DeRuntz [4], and Hughes and Liu [5,6]. The procedure is amenable to a root-amplification stability analysis that eliminates the need for ad-hoc investigation of special partitions. Below we summarize the equations from [1] that will be needed for the ensuing exposition.

Equations of Motion:

$$\underset{\sim}{M}\,\ddot{\underline{u}} + \underset{\sim}{D}\,\dot{\underline{u}} + \underset{\sim}{K}\,\underline{u} = \underline{f} \tag{1}$$

Implicit Integrator:

$$\begin{cases} \underline{u}_n = \delta\,\dot{\underline{u}}_n + \underline{h}^u_n \\ \underline{h}^u_n = \displaystyle\sum_{j=1}^{m} (\alpha_j\,\underline{u}_{n-j} - \delta\,\beta_j\,\dot{\underline{u}}_{n-j}) \end{cases} \tag{2}$$

Implicit Difference Equations:

$$\begin{cases} \underset{\sim}{E}\,\underline{u}_n = \underline{g}_n \\ \underset{\sim}{E} = \underset{\sim}{M} + \delta\,\underset{\sim}{D} + \delta^2\,\underset{\sim}{K} \\ \underline{g}_n = \delta^2\,\underline{f}_n + \underset{\sim}{M}\,(\underline{h}^u_n + \delta\,\underline{h}^{\dot{u}}_n) \end{cases} \tag{3}$$

Partitioned Difference Equations:

$$\left\{\begin{array}{l} \underset{\sim}{D} = \underset{\sim}{D}_1 + \underset{\sim}{D}_2 \\ \underset{\sim}{K} = \underset{\sim}{K}_1 + \underset{\sim}{K}_2 \\ E = E_1 + E_2 \\ \underset{\sim}{E}_1 = \underset{\sim}{M} + \delta \underset{\sim}{D}_1 + \delta^2 \underset{\sim}{K}_1 \\ \underset{\sim}{E}_2 = \delta \underset{\sim}{D}_2 + \delta^2 \underset{\sim}{K}_2 \\ \underset{\sim}{E}_1 \underline{u}_n = \underline{g}_n - \underset{\sim}{E}_2 \underline{u}_n^{(p)} \end{array}\right. \qquad (4)$$

In the foregoing equations, $\underset{\sim}{M}$, $\underset{\sim}{D}$ and $\underset{\sim}{K}$ are mass, damping and stiffness matrices, respectively; $\underline{u}$ and $\underline{f}$ are solution and applied-force N-vectors, respectively; dot superscript denote temporal differentiation; δ is a generalized time stepsize, α_j and β_j are coefficients of the linear multistep integration formula used, and $\underline{h}^u$ is the corresponding historical vector; $\underline{u}^{(p)}$ denotes predicted or extrapolated solution vector. Subscript n indicates computed values pertaining to the sample time $t = t_n$. Finally, subscripts 1 and 2 identify terms associated with the sum-partition of matrices $\underset{\sim}{D}$ and $\underset{\sim}{K}$.

Table 1 provides a set of examples of specific partitions of the stiffness matrix $\underset{\sim}{K}$ tailored to a coupled mechanical system consisting of two fields: x and y, which interact through a boundary b.

TABLE 1. EXAMPLES OF PARTITIONS FOR TWO-FIELD PROBLEMS

Node-by-Node	Element-by-Element	DOF-by-DOF	Staggered
$\underset{\sim}{K}_2 = \begin{bmatrix} 0 & 0 & 0 \\ 0 & 0 & 0 \\ 0 & \underset{\sim}{K}_{yb} & \underset{\sim}{K}_{yy} \end{bmatrix}$	$\underset{\sim}{K}_2 = \begin{bmatrix} 0 & 0 & 0 \\ 0 & \underset{\sim}{K}^{y}_{bb} & \underset{\sim}{K}_{by} \\ 0 & \underset{\sim}{K}_{yb} & \underset{\sim}{K}_{yy} \end{bmatrix}$	$\underset{\sim}{K}_2 = \begin{bmatrix} 0 & 0 & 0 \\ 0 & 0 & 0 \\ 0 & 0 & \underset{\sim}{K}_{yy} \end{bmatrix}$	$\underset{\sim}{K}_2 = \begin{bmatrix} 0 & 0 & 0 \\ 0 & 0 & 0 \\ 0 & \underset{\sim}{K}_{yb} & 0 \end{bmatrix}$

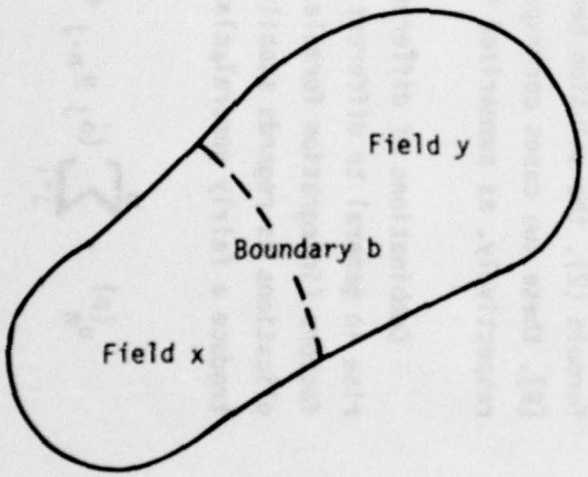

Coupled Field Stiffness-Matrix

$$\underset{\sim}{K} = \begin{bmatrix} \underset{\sim}{K}_{xx} & \underset{\sim}{K}_{xb} & 0 \\ \underset{\sim}{K}_{bx} & \underset{\sim}{K}^{x}_{bb} + \underset{\sim}{K}^{y}_{bb} & \underset{\sim}{K}_{by} \\ 0 & \underset{\sim}{K}_{yb} & \underset{\sim}{K}_{yy} \end{bmatrix}$$

$$\underset{\sim}{K} = \underset{\sim}{K}_1 + \underset{\sim}{K}_2$$

EFFECT OF COMPUTATIONAL PATH AND EXTRAPOLATOR SELECTION

Ref. [8] discussed the organization of the time-advancing calculations and identified four "computational paths", which were labeled (0'), (0), (1) and (2). Paths differ according to the way in which auxiliary quantities such as velocities are calculated. In [1] it was shown that computational paths can have a significant effect on the stability of partitioned solution procedures, and that this effect is tied up with the selection of extrapolators. For example, when the trapezoidal integration rule is used in conjunction with the last-solution extrapolator,

$$\underline{u}_n^{(p)} = \underline{u}_{n-1} \tag{5}$$

the solution remains stable if the velocity is computed by integrating the acceleration that is in turn obtained from the equations of motion. On the other hand, if the velocity is computed from the difference formula (2), the solution becomes unstable. In terms of the nomenclature of [8], these two cases correspond to the (C0') and the (C1)-computational path, respectively, as summarized in Table 2.

Combinations of different extrapolators and computational paths will give rise in general to different characteristic equations, even if all other factors (integration formula, partition) remain the same. This has major implications as regards stability and accuracy. To study these effects, we introduce a fairly general class of extrapolators:

$$u_n^{(p)} = \sum_{j=1}^{m} (\hat{\alpha}_j \underline{u}_{n-j} + \delta \hat{\beta}_j \dot{\underline{u}}_{n-j} + \delta^2 \hat{\gamma}_j \ddot{\underline{u}}_{n-j}) \tag{6}$$

TABLE 2. COMPUTATIONAL PATH-DEPENDENT FORMULAS FOR PARTITIONED PROCEDURES

$(\underset{\sim}{E}_1 \cdot \underline{u}_n = \underline{g}_n - \underset{\sim}{E}_2 \cdot \underline{u}_n^{(p)})$

Computational Path	Computational Sequences	Recommended Predictor, $\underline{u}_n^{(p)}$
(CO')	a $\underline{g}_n = (\underset{\sim}{M} + \delta \underset{\sim}{D})\,\underline{h}_n^{u} + \delta \underset{\sim}{M}\,\underline{h}_n^{\dot{u}} + \delta^2 \underline{f}_n$ b $\underline{u}_n = \underset{\sim}{E}_1^{-1}(\underline{g}_n - \underset{\sim}{E}_2 \cdot \underline{u}_n^{(p)})$ c $\dot{\underline{u}}_n = (\underline{u}_n - \underline{h}_n^{u})/\delta$ d $\ddot{\underline{u}}_n = \underset{\sim}{M}^{-1}(\underline{f}_n - \underset{\sim}{D}\,\dot{\underline{u}}_n - \underset{\sim}{K}\,\underline{u}_n)$ e $\dot{\underline{u}}_n = \delta\,\ddot{\underline{u}}_n + \underline{h}_n^{\dot{u}}$	1) $\sum_{j=1}^{m} -\alpha_j \underline{u}_{n-j}$ 2) $\sum_{j=1}^{m} [-\alpha_j \underline{u}_{n-j} + \delta(\beta_j/\beta_o - \alpha_j)\dot{\underline{u}}_{n-j} + \delta^2(\beta_j/\beta_o - \alpha_j)\ddot{\underline{u}}_{n-j}]$ †
(C1)	a-d same as (CO'), e skipped	$\sum_{j=1}^{m} [-\alpha_j \underline{u}_{n-j} + \delta(\beta_j/\beta_o - \alpha_j)\dot{\underline{u}}_{n-j}$
(C2)	a-c same as (CO'), d $\ddot{\underline{u}}_n = (\dot{u}_n - \underline{h}_n^{\dot{u}})/\delta$ e skipped	$\sum_{j=1}^{m} [-\alpha_j \underline{u}_{n-j} + \delta(\beta_j/\beta_o - \alpha_j)\dot{\underline{u}}_{n-j} + \delta^2 \beta_j/\beta_o \ddot{\underline{u}}_{n-j}]$
(J0)	a $\underline{g}_n = \underset{\sim}{M}\,\underline{h}_n^{u} + \delta\,\underline{h}_n^{v} + \alpha^2 \underline{f}_n$ b-c same as (CO') d $\dot{\underline{v}}_n = \underline{f}_n - \underset{\sim}{K}\,\underline{u}_n$ e $\underline{v}_n = \delta\,\dot{\underline{v}}_n + \underline{h}_n^{v}$	$\sum_{j=1}^{m} [-\alpha_j \underline{u}_{n-j} + \delta\,\beta_j/\beta_o \dot{\underline{u}}_{n-j}]$

† Predictor (2) in the Path (CO') case is recommended for implicit-explicit procedures when accuracy, including rigid-body motions becomes important. In this case stability limit is somewhat reduced.

TABLE 3. COMPUTATIONAL PATH-DEPENDENT CHARACTERISTIC EQUATIONS ($\underset{\sim}{D} = \underset{\sim}{0}$)

Implementation Path	Characteristic Equation
CO'	$\lvert \rho^2 \underset{\sim}{M} + \delta^2 \sigma^2 \underset{\sim}{K}_1 + \delta^2 (e_0 \rho + \sigma^2 - \rho \lambda^m) \underset{\sim}{K}_2 - \delta^4 (e_1 \sigma + e_2 \rho) \underset{\sim}{K}_2^{-1} \underset{\sim}{K} \rvert = 0$
C1	$\lvert \rho^2 \underset{\sim}{M} + \delta^2 \sigma^2 \underset{\sim}{K}_1 + \delta^2 (\sigma e_0 + \sigma^2 - \sigma \lambda^m + \rho e_1) \underset{\sim}{K}_2 - \delta^4 e_2 \underset{\sim}{K}_2 M^{-1} \underset{\sim}{K} \rvert = 0$
C2	$\lvert \rho^2 \underset{\sim}{M} + \delta^2 \sigma^2 \underset{\sim}{K}_1 + \delta^2 (\sigma^2 e_0 + \rho \sigma e_1 + \rho^2 e_0) \underset{\sim}{K}_2 \lambda^m \rvert = 0$
JO	$\lvert \lambda^m \rho^2 \underset{\sim}{M} + \delta^2 \lambda^m \sigma^2 \underset{\sim}{K}_1 + \delta^2 (\sigma^2 \lambda^m + e_0 \rho \sigma + e_1 \rho^2) \underset{\sim}{K}_2 - \delta^4 \sigma e_2 \underset{\sim}{K}_2 \underset{\sim}{M}^{-1} \underset{\sim}{K} \rvert = 0$

In the above equations, ρ, σ, e_1 and e_2 are given by:

$$\begin{cases} \rho(\lambda) = \sum_{j=0}^{m} \alpha_j \lambda^{m-j} \\ \sigma(\lambda) = \sum_{j=0}^{m} \beta_j \lambda^{m-j} \\ e_0 (e_1, e_2) = \sum_{j=1}^{m} \hat{\alpha}_j (\hat{\beta}_j, \hat{\gamma}_j) \lambda^{m-j} \end{cases}$$

$$\lambda = (1 + z)/(1 - z)$$

where $\hat{\alpha}_j$, $\hat{\beta}_j$ and $\hat{\gamma}_j$ are numeric coefficients. This class is broader than that considered in [1], which did not account for historical derivative terms $\underline{\hat{u}}_{n-j}$, $\underline{\ddot{u}}_{n-j}$.

The characteristic matrix equations for the four computational sequences of Table 2 can be derived by seeking nontrivial solutions of the form

$$u_k = \lambda^k u_o = \left(\frac{1+z}{1-z}\right)^k u_o \tag{7}$$

The resulting formulas are collected in Table 3. An undamped system ($\underset{\sim}{D} = \underset{\sim}{0}$) is assumed for simplicity; the damped case can be handled in a similar fashion. For derivation details Appendix A of [1] should be consulted.

Numerical stability requires

$$\mathrm{Re}(z_i) \leq 0, \quad i = 1, \ldots 2\,Nm \tag{8}$$

for each characteristic equation in Table 3. This imposes in turn constraints on the selection of extrapolators for each path; recommended extrapolators are listed in Table 2. For the important case of the trapezoidal integration rule, stable extrapolators are listed in Table 4.

Remark: If partitioning is performed at the differential equation level as opposed to the present difference equation level, viz.,

$$\underset{\sim}{M}\,\ddot{\underline{u}} + \underset{\sim}{D}_1\,\hat{\underline{u}} + \underset{\sim}{K}_1\,\underline{u} = \underline{f} - \underset{\sim}{D}_2\,\hat{\underline{u}} - \underset{\sim}{K}_2\,\underline{u} \tag{9}$$

the following characteristic equation results with $\underset{\sim}{D} = \underset{\sim}{0}$

$$\det\left|\rho^2\,\underset{\sim}{M} + \delta^2\,\underset{\sim}{K}_1 + \delta^2\left(\sigma^2 e_1 + \rho\,\sigma\,e_1 + \rho^2 e_2\right)\underset{\sim}{K}_2\right| = 0 \tag{10}$$

TABLE 4. STABLE EXTRAPOLATORS FOR DIFFERENT COMPUTATIONAL PATHS FOR TRAPEZOIDAL INTEGRATION FORMULA

Computational Path	Stable Extrapolator
(CO')	$u_n^{(p)} = \begin{cases} u_{n-1}^{\bullet} \\ (u_{n-1} + h\,\dot{u}_{n-1} + \frac{h^2}{2}\,\ddot{u}_{n-1})^{\dagger} \end{cases}$
(C1)	$u_n^{(p)} = u_{n-1} + h\,\dot{u}_{n-1}$
(C2)	$u_n^{(p)} = u_{n-1} + h\,\dot{u}_{n-1} + \frac{h^2}{4}\,\ddot{u}_{n-1}$
(JO)	$u_n^{(p)} = u_{n-1} + \frac{h}{2}\,\dot{u}_{n-1}$

* This is used extensively in [1].

† Applicable strictly to implicit-explicit partitions with somewhat reduced stability limits, e.g., $\omega_{max} \cdot h \leq 1.57$ for DOF-by-DOF I - E partitions.

Integrator: $u_n = u_{n-1} + \delta(\dot{u}_n + \dot{u}_{n-1}),\ \delta = \frac{h}{2}$

Extrapolator Form: $u_n^{(p)} = u_{n-1} + \hat{\beta}\,\delta\,\dot{u}_{n-1} + \hat{\gamma}\,\delta^2\,\ddot{u}_{n-1}$

which is independent of the computational path. It can be proved that, when the trapezoidal rule is used, the differential partitioning procedure (9) is stable provided the extrapolator is chosen in the form

$$\underline{u}_n^{(p)} = \underline{u}_{n+1} + h\,\dot{\underline{u}}_{n-1} + \frac{h^2}{4}\,\ddot{\underline{u}}_{n-1} \tag{11}$$

in which $\dot{\underline{u}}$ and $\ddot{\underline{u}}$ are computed by differentiation formulas regardless of the the implementation paths adopted. The above extrapolator for the differential partitioning procedure (9) is identical to that of path (C2) for the algebraic partitioning procedure (4) (see Table 4). Hence, it appears that computational advantages of the (J0), (C0'), (C0) and (C1) computational paths are negated in the differential partitioning, whereas they are preserved in the algebraic partitioning.

PRESERVATION OF RIGID BODY MOTIONS

The spatial convergence of nonconforming finite elements has been traditionally tested with Irons' patch test [9], which among other things verifies whether rigid body motions are accurately represented. In a similar vein, for partitioned solution procedures it is important to check which combination of extrapolator and computational paths preserves rigid-body motions. Note that if the temporal order of accuracy of the implicit integration formula is two, so is that of partitioned difference equation (4a). Thus, one is tempted to believe that procedures of formally second-order accuracy should trace constant velocity and constant-acceleration motions as they vary linearly and quadratically in time, respectively. The formal order of accuracy holds true, however, only for solution components that are not on the partitioned boundaries (see Table 1). Hence, the partition (4a) does not in general preserve the two practically important rigid-body motions. A notable exception to this statement occurs for those partitions whose K_2 matrix admits rigid body motions. These effects will now be examined assuming that the trapezoidal integration rule is used.

Rigid body motions $\underline{u}$ of a flexible structure satisfy

$$\underset{\sim}{K}\,\underline{u} = 0 \tag{12}$$

Introducing the partition (4e):

$$\underset{\sim}{K}_1\,\underline{u} = -\underset{\sim}{K}_2\,\underline{u} \tag{13}$$

Now equation (13) implies that

$$(\underset{\sim}{M} + \delta^2\,\underset{\sim}{K}_1)\,\underline{u} = (\underset{\sim}{M} - \delta^2\,\underset{\sim}{K}_2)\,\underline{u} \tag{14}$$

If computational path (0') is followed, the following difference equation holds (cf. Table 2):

$$(\underset{\sim}{M} + \delta^2 \underset{\sim}{K}_1)\, \underline{u}_n = \delta^2 \underline{f}_n + \underset{\sim}{M}(\underline{u}_{n-1} + 2\delta^2 \ddot{\underline{u}}_{n-1} - \delta^2 \underset{\sim}{K}_2 \underline{u}^P_{n-1} \tag{15}$$

For a constant-acceleration rigid-body motion, we must have

$$\underset{\sim}{M}\, \ddot{\underline{u}}_k = \underline{f}_k\,, \quad k = 0, 1 \ldots \tag{16}$$

Inserting (16) into (15) and accounting for (14), it follows that exactness of representation demands that either $\underset{\sim}{K}_2 \underline{u}_n \equiv \underline{0}$ or that the following predictor be used

$$\underline{u}^P_n = \underline{u}_{n-1} + 2\delta\, \dot{\underline{u}}_{n-1} + 2\delta^2 \ddot{\underline{u}}_{n-1} \tag{17}$$

This is the second predictor formula given for path (0') in Table 3.

Remark 1. If one insists only on exact preservation of constant velocity rigid body motions, for which $\ddot{\underline{u}}_n \equiv \underline{0}$, the following predictors can be used:

$$\underline{u}^P_n = \underline{u}_{n-1} + 2\delta\, \dot{\underline{u}}_{n-1} \tag{18}$$

$$\underline{u}^P_n = \underline{u}_{n-1} + 2\delta\, \dot{\underline{u}}_{n-1} + \delta^2 \ddot{\underline{u}}_{n-1}$$

Remark 2. Both the element-by-element and node-by node partitions preserve any rigid-body motions because these two partitions satisfy the rigid-body conserving identity

$$\underset{\sim}{K}_1 \underline{u}_n = \underset{\sim}{K}_2 \underline{u}_n = \underline{0} \tag{19}$$

For these partitions, the last-solution extrapolator $\underline{u}_n^p = \underline{u}_{n-1}$ is optimally stable for path (0') and preserves rigid-body motions. For other computational paths, the equivalent predictors listed in Table 2 retain these properties.

Remark 3. The last-solution extrapolator, although stable, distorts constant velocity and constant-acceleration rigid body motions for the DOF-by-DOF and staggered partitions. This effect is illustrated in Figure 1 for a two degree-of-freedom problem. This distortion can only be eliminated by iterating at each time step to convergence.

Remark 4. The accurate extrapolator (17) gives rise to numerical instability for paths other than (0'). Thus, stability and accuracy (as far as preservation of rigid body motions is concerned) are not generally equivalent attributes for partitioned integration.

The main findings of this study are summarized in Table 5. Clearly path (0') is the choice when accurate representation of constant-acceleration rigid-body motions is important, and a DOF-by-DOF partition is used. The price paid for this formulation is the need for additional calculations, such as solving for accelerations, in the advancing step [8]. If the accuracy requirement is relaxed to preservation of constant-velocity rigid-body motions, then either path (1) or (2) is acceptable for those partitions (because predictors (18a) and (18b) are stable for those paths, cf. Table 2), and the computational effort is accordingly reduced. Finally, path (0) distorts rigid body motions other than constant displacement for the DOF-by-DOF and staggered partitions.

So far we have focused our attention on the construction of stable and accurate extrapolators and on conditions for preserving rigid-body motions. The remainder of the paper will be devoted to the examination of the "incremental" effect of partition on algorithmic accuracy.

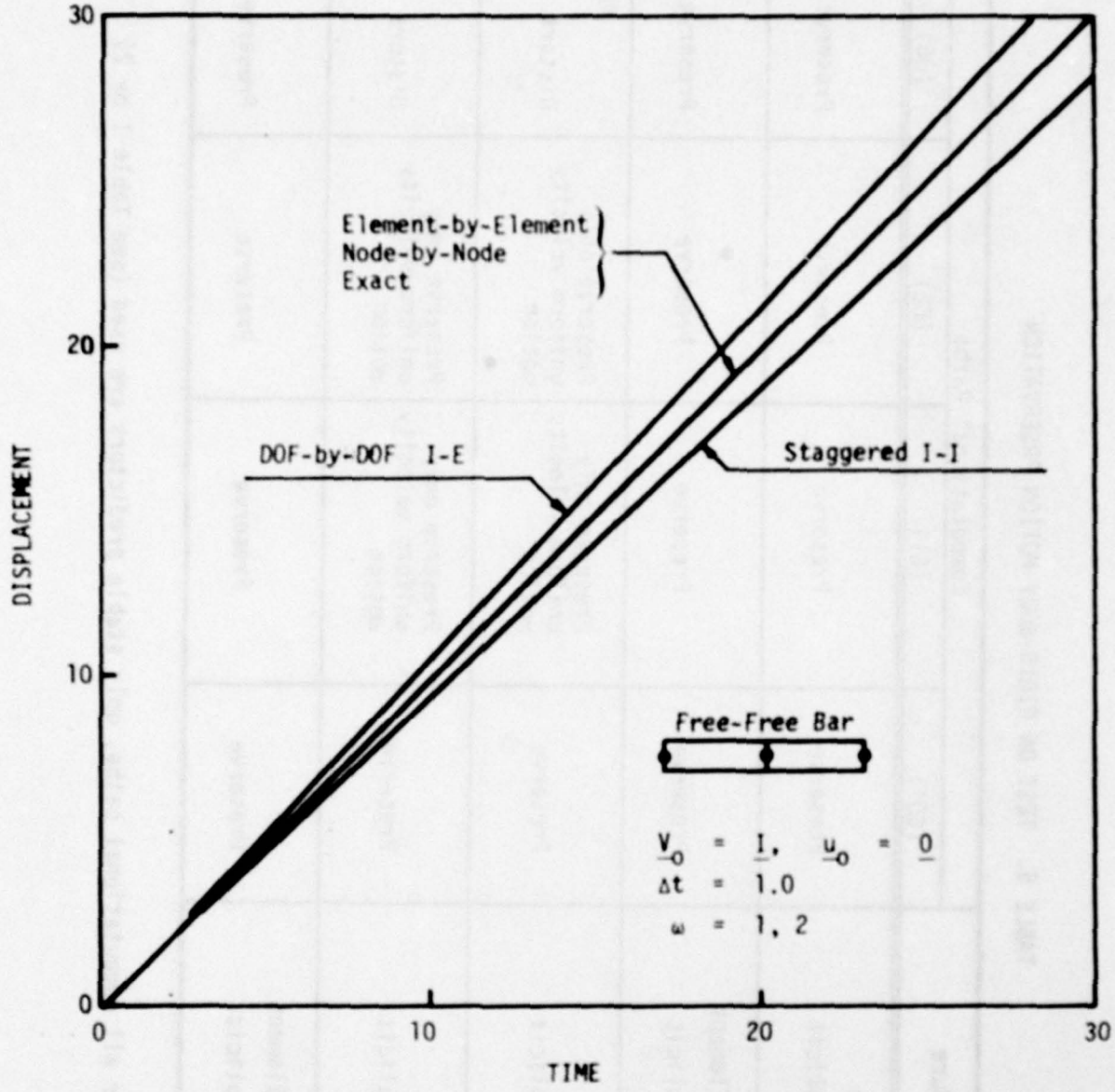
30
20
10
0
0
10
20
30
DISPLACEMENT
TIME
Element-by-Element
Node-by-Node
Exact
DOF-by-DOF I-E
Staggered I-I
Free-Free Bar
$\underline{V}_o = \underline{1}, \quad \underline{u}_o = \underline{0}$
$\Delta t = 1.0$
$\omega = 1, 2$

Figure 1

TABLE 5. TEST ON RIGID-BODY MOTION PRSERVATION

Procedure	Computational Paths			
	(C0')	(C1)	(C2)	(J0)
Node-by-Node Implicit-Explicit	Preserve	Preserve	Preserve	Preserve
Element-by-Element Implicit-Explicit	Preserve	Preserve	Preserve	Preserve
DOF-by-DOF Implicit-Explicit	Preserve	Preserve only uniform velocity motion	Preserve only uniform velocity motion	Distort
Staggered Implicit-Implicit	Preserve	Preserve only uniform velocity motion	Preserve only uniform velocity motion	Distort
Element-by-Element Implicit-Implicit	Preserve	Preserve	Preserve	Preserve

Remark: For all computational paths, only stable predictors are used (see Table 1 or 2)

EFFECT OF PARTITIONING ON ALGORITHMIC ACCURACY

The conventional Fourier technique for assessing accuracy of integration formulas for second-order systems proceeds as follows. First, the homogeneous difference equations are decoupled by projecting them on normal coordinates. Second, the frequency distortion and numerical damping of an uncoupled difference equation subjected to harmonic input of frequency ω are presented as functions of the normalized sampling frequency ωh. This procedure is not immediately applicable to the partitioned difference equations (4b), however, because these are not generally diagonalized by the normal modes of the semidiscrete equations (1).

In this paper a limit differential equation approach will be utilized to assess the frequency-dependent accuracy of various partitioned procedures, assuming that the solutions can be expanded in Taylor series up to the order of the integration formula. This approach has been extensively used for the evaluation of artificial viscosity [10,11]. It will be shown that the limit differential equations for the partitioned difference equations display a frequency distortion effect as primary error source due to partitioning.

As an illustration when the trapezoidal formula is used in conjunction with path (CO') and the previous solution vector $\underline{u}_{n-1}$ is used as the extrapolator, the following limit differential equations can be derived (see, for example, Roache [11] for details),

$$(\underset{\sim}{M} - \frac{2}{3}\delta^2 \underset{\sim}{K}_1 + \frac{1}{3}\delta^2 \underset{\sim}{K}_2)\,\ddot{\underline{u}} + \underset{\sim}{K}\,\underline{u} = \underline{0}(\delta^3) \qquad (19)$$

Note that the mass matrix is considerably modified whereas the stiffness matrix is not, and also the absence of terms associated with the velocity vector $\dot{\underline{u}}$. We therefore conclude that the primary additional algorithmic error caused by partitioning is manifested in the frequency distortion,

which has to be evaluated from its frequency equation

$$\det \left| \left(\underset{\sim}{M} - \frac{2}{3}\delta^2 \underset{\sim}{K}_1 + \frac{1}{3}\delta^2 \underset{\sim}{K}_2 \right) \Omega^2 - \delta^2 \underset{\sim}{K} \right| = 0 , \quad \Omega = \omega \delta \tag{20}$$

The two limit cases for (20) are: $\underset{\sim}{K}_2 = 0$ (fully implicit integration) and $\underset{\sim}{K}_2 = \underset{\sim}{K}$ (fully explicit integration). These correspond in turn to the standard trapezoidal rule and central difference formula, respectively. It is well known that these two formulas introduce no numerical damping. Moreover, the central difference formula shortens the period whereas the trapezoidal rule elongates it by an amount roughly twice as big; this can be immediately deduced from (20). That the frequency distortion is also the primary algorithmic error due to partitioning can also be shown to be true for other, numerically damped, integration formulas. (The demonstration relies on the fact that nonzero odd-derivative residual terms in the Taylor series occur beyond the order of the integration formula truncation error).

As noted previously, the matrix equation (19) is not generally diagonalizable by the natural modes of the original equations of motion. To assess the accuracy performance of various partitions we can exploit, however, the fact that the frequency error due to partitioning emanates from partition boundaries. This enables us to construct a two degree-of-freedom model system and to assess the fequency distortion due to partitioning from that of the model system. The governing equations of this system are

$$\begin{bmatrix} 1+\alpha & 0 \\ 0 & 1 \end{bmatrix} \ddot{\underline{u}} + \begin{bmatrix} 1+\frac{1}{\alpha} & -1 \\ -1 & 1 \end{bmatrix} \underline{u} = \underline{0} \tag{21}$$

with appropriate initial conditions. Equations (21) can be viewed as the axial equations of motion for a fixed-free bar consisting of two elements whose length ratio is $1:\alpha$.

For the above two-d.o.f. system the partition-caused artificial frequency distortion can be evaluated by equation (20). Alternatively, the

distortion can be computed exactly from the characteristic equation for the partitioned difference equations (see Table 3). As the calculations by the two approaches have shown no discernible difference, we present the frequency distortion by the latter approach in the sequel.

Figures 2a and 2b show the frequency distortion of the low and high frequency components for the equal length case $\alpha = 1$. For this case the node-by-node implicit-explicit procedure is the most accurate, followed by the element-by-element, the DOF-by-DOF, and the staggered procedures. As the element length ratio (roughly square of the frequency ratio) is decreased, however, an intermediate value of α is reached at which the element-by-element procedure becomes more accurate than the node-by-node procedure (see Fig. 3). If the length ratio is further decreased, the low (high) frequency error approaches that of fully explicit (implicit) formula, respectively, as can be shown from Figure 4. The increase in the frequency ratio weakens the coupling effect between the two

From the foregoing accuracy analysis of the model system it can be seen that accuracy of solution components far from the partition boundaries is largely controlled by that of the integration formulas used. For solution components at or near the partition boundaries, the element-by-element and the node-by-node partitions enjoy a somewhat higher accuracy than either the explicit or the implicit formula itself in the sense that the frequency distortions are less than those of the fully explicit (implicit) integration formulas (see Figs. 2 and 3). On the other hand, for the DOF-by-DOF and the staggered partitions the accuracy of the boundary solution components is inferior to that of the fully explicit (implicit) formulas.

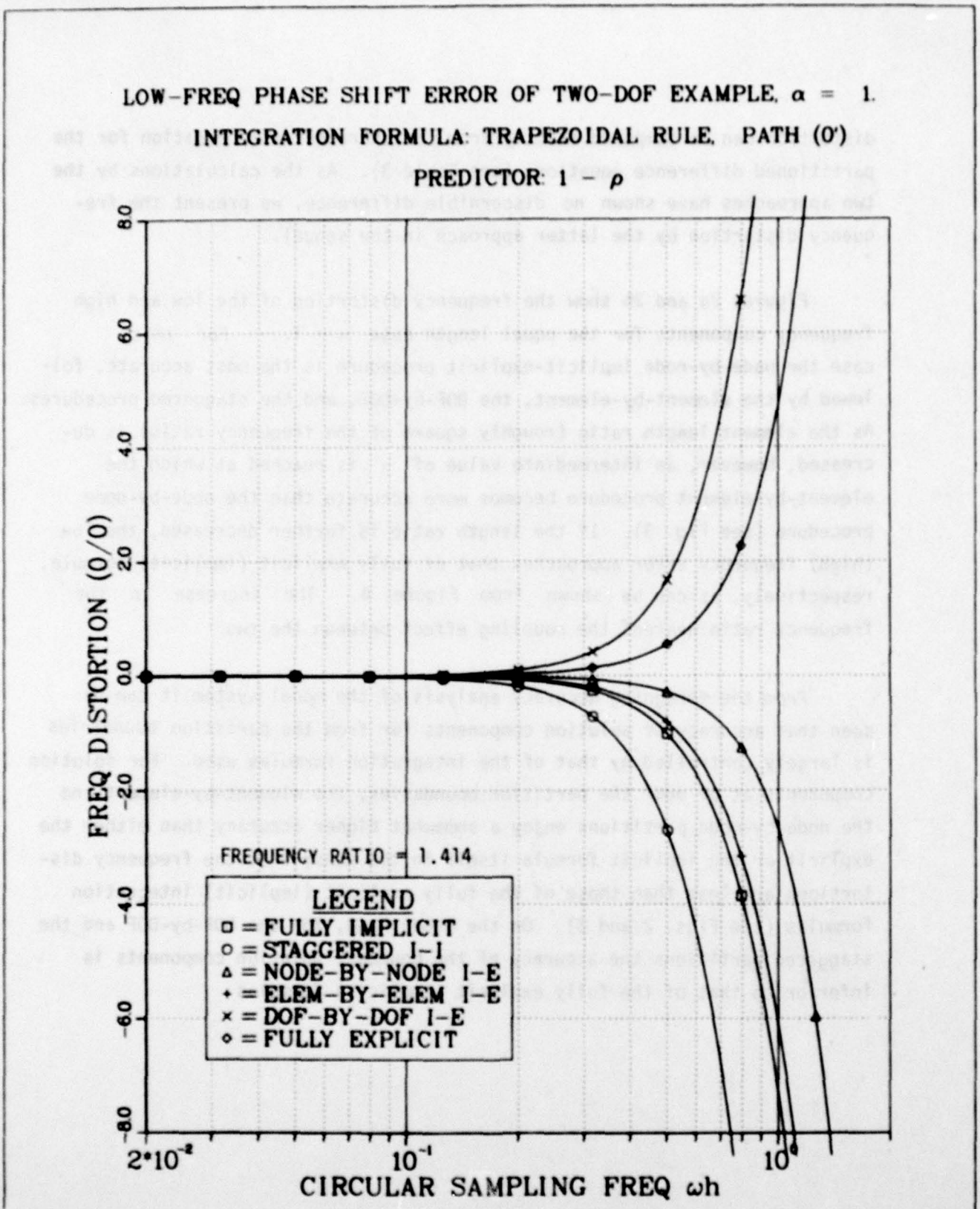
LOW-FREQ PHASE SHIFT ERROR OF TWO-DOF EXAMPLE, α = 1.
INTEGRATION FORMULA: TRAPEZOIDAL RULE, PATH (0')
PREDICTOR: 1 − ρ
FREQ DISTORTION (0/0)
80
60
40
20
0.0
-20
-40
-60
-80
FREQUENCY RATIO = 1.414
LEGEND
□ = FULLY IMPLICIT
○ = STAGGERED I-I
△ = NODE-BY-NODE I-E
• = ELEM-BY-ELEM I-E
× = DOF-BY-DOF I-E
◇ = FULLY EXPLICIT
2*10^-2
10^-1
10^0
CIRCULAR SAMPLING FREQ ωh

Figure 2a

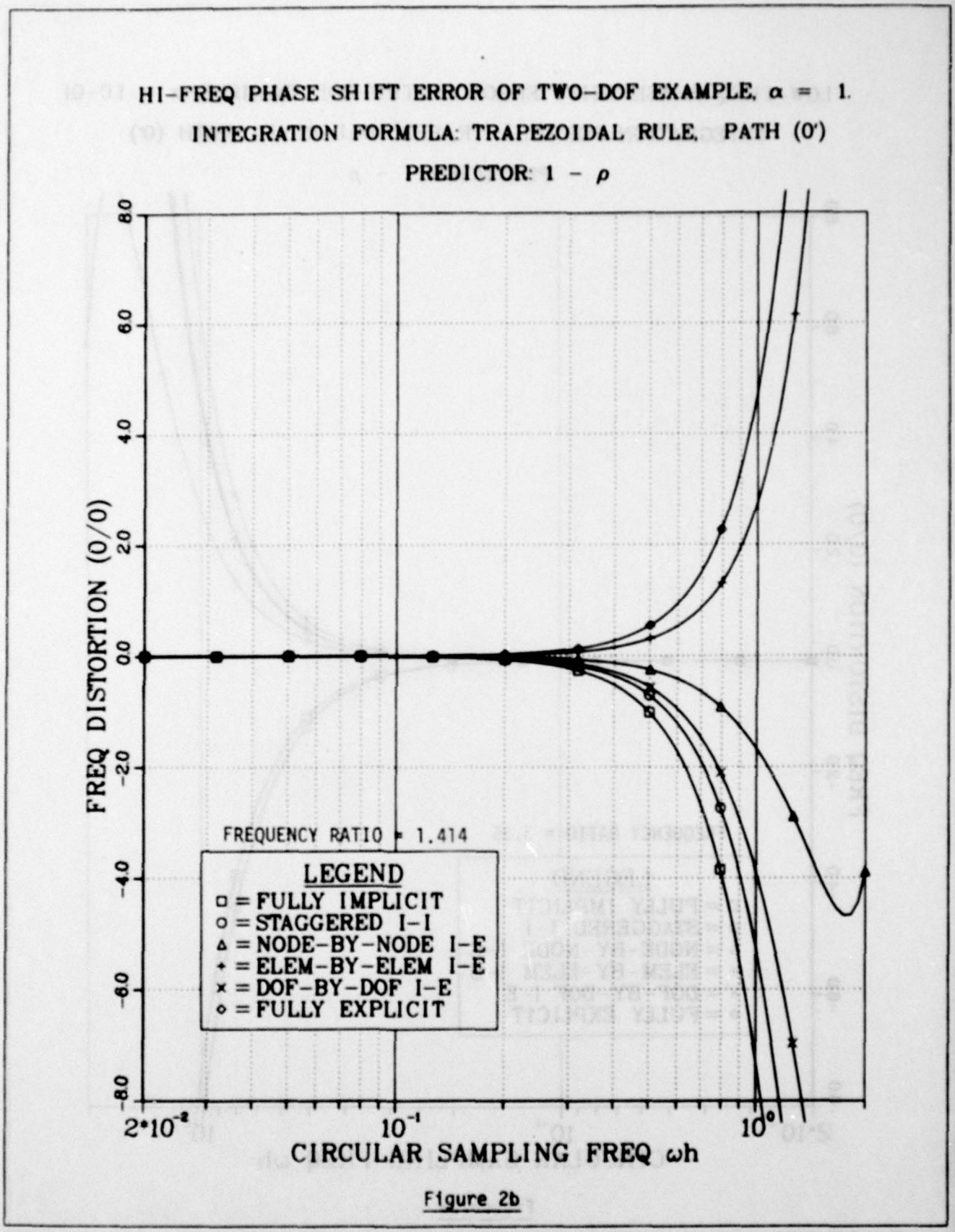
HI-FREQ PHASE SHIFT ERROR OF TWO-DOF EXAMPLE, α = 1.
INTEGRATION FORMULA: TRAPEZOIDAL RULE, PATH (0')
PREDICTOR: 1 - ρ
FREQ DISTORTION (0/0)
80
60
40
20
0.0
-20
-40
-60
-80
FREQUENCY RATIO = 1.414
LEGEND
□ = FULLY IMPLICIT
○ = STAGGERED I-I
△ = NODE-BY-NODE I-E
+ = ELEM-BY-ELEM I-E
× = DOF-BY-DOF I-E
◇ = FULLY EXPLICIT
2*10⁻²
10⁻¹
10⁰
CIRCULAR SAMPLING FREQ ωh

Figure 2b

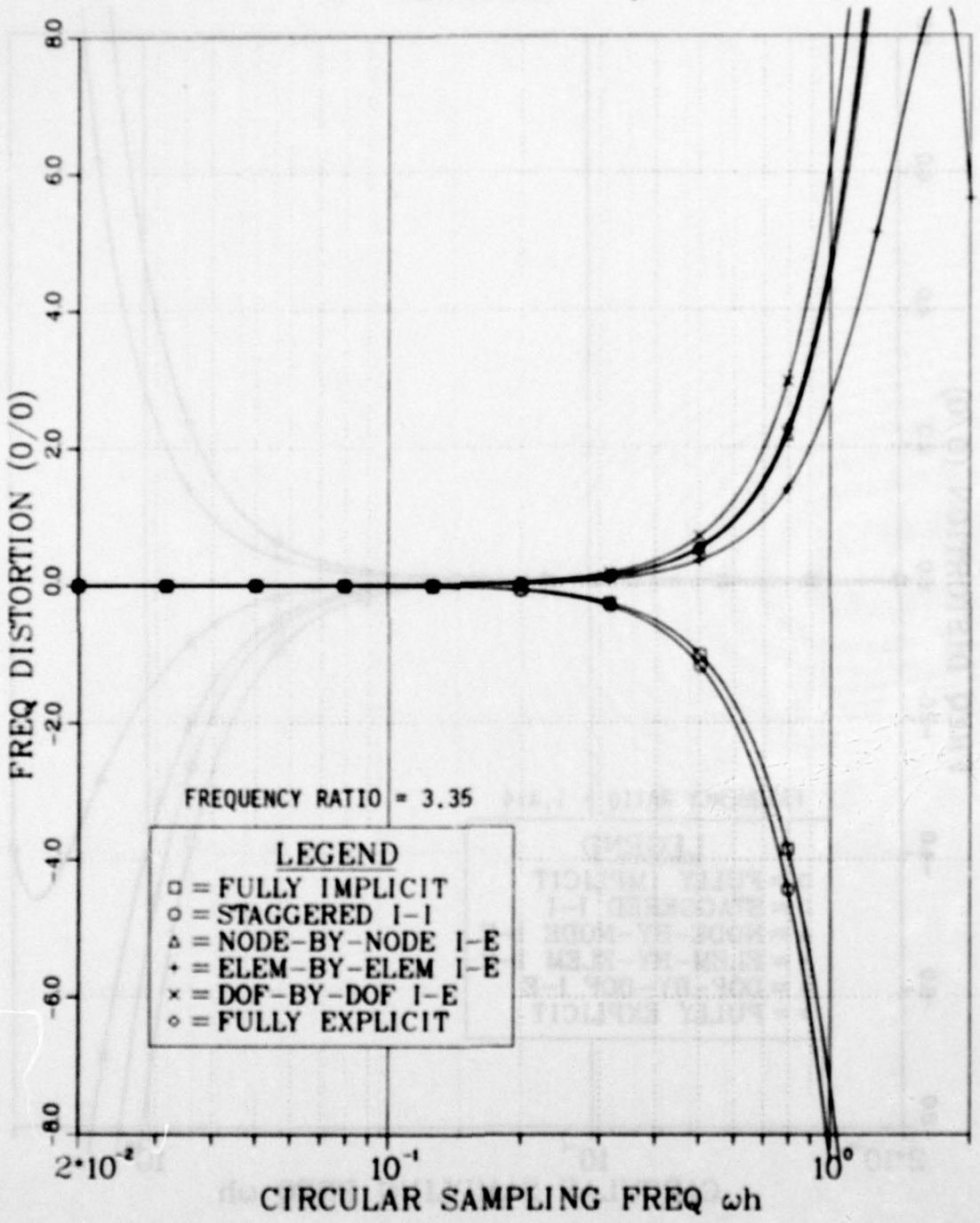
LOW-FREQ PHASE SHIFT ERROR OF TWO-DOF EXAMPLE α = 1.0-01
INTEGRATION FORMULA: TRAPEZOIDAL RULE, PATH (0')
PREDICTOR: 1 - ρ
FREQ DISTORTION (0/0)
80
60
40
20
00
-20
-40
-60
-80
FREQUENCY RATIO = 3.35
LEGEND
□ = FULLY IMPLICIT
○ = STAGGERED I-I
△ = NODE-BY-NODE I-E
• = ELEM-BY-ELEM I-E
× = DOF-BY-DOF I-E
◇ = FULLY EXPLICIT
2*10⁻²
10⁻¹
10⁰
CIRCULAR SAMPLING FREQ ωh

Figure 3a

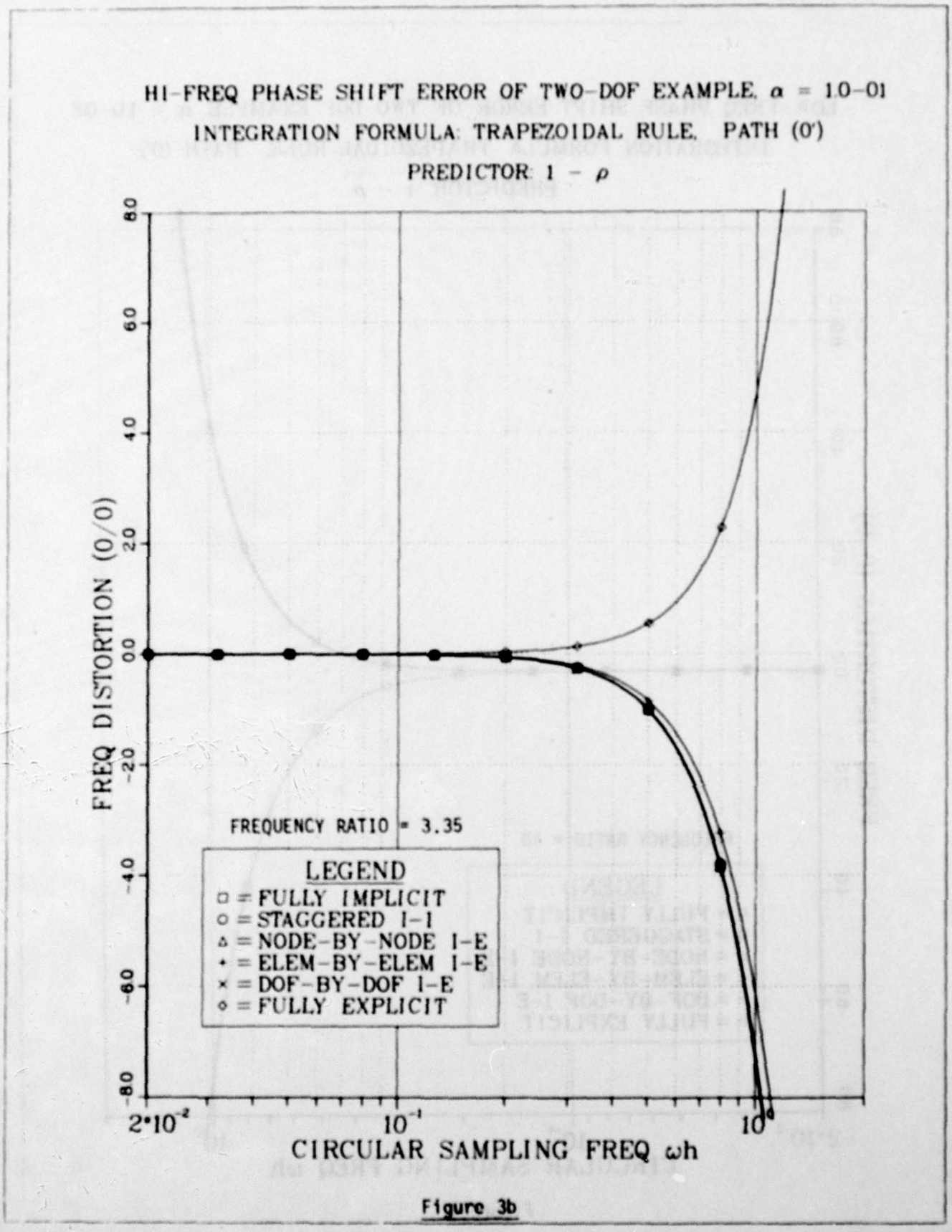
HI-FREQ PHASE SHIFT ERROR OF TWO-DOF EXAMPLE. α = 1.0-01
INTEGRATION FORMULA: TRAPEZOIDAL RULE. PATH (0')
PREDICTOR: 1 - ρ
FREQ DISTORTION (0/0)
80
60
40
20
00
-20
-40
-60
-80
FREQUENCY RATIO = 3.35
LEGEND
□ = FULLY IMPLICIT
○ = STAGGERED I-I
△ = NODE-BY-NODE I-E
• = ELEM-BY-ELEM I-E
× = DOF-BY-DOF I-E
◇ = FULLY EXPLICIT
2*10^-2
10^-1
10^0
CIRCULAR SAMPLING FREQ ωh

Figure 3b

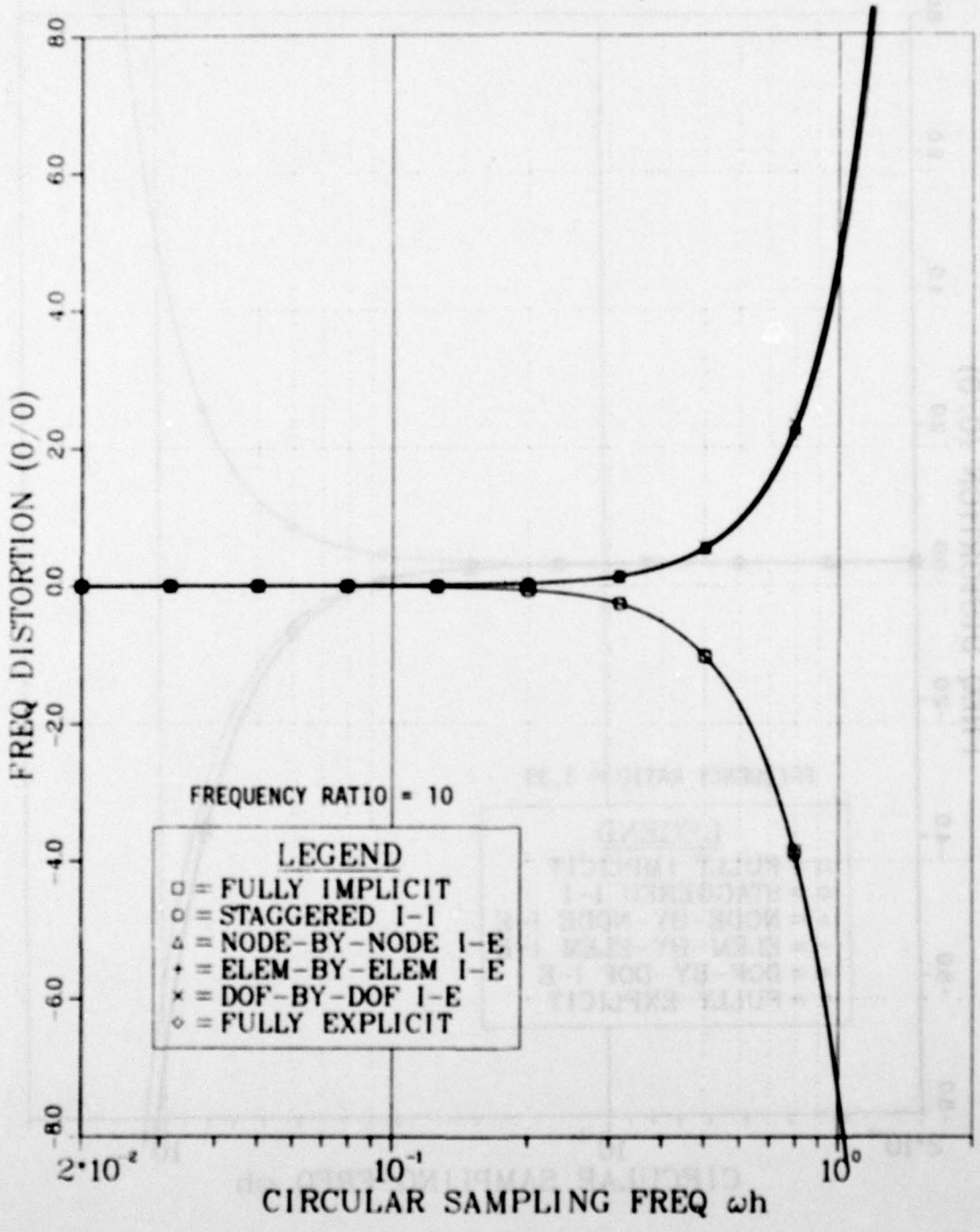
LOW-FREQ PHASE SHIFT ERROR OF TWO-DOF EXAMPLE, α = 1.0-02
INTEGRATION FORMULA: TRAPEZOIDAL RULE, PATH (0')
PREDICTOR: 1 - ρ
FREQ DISTORTION (0/0)
80
60
40
20
00
-20
-40
-60
-80
FREQUENCY RATIO = 10
LEGEND
□ = FULLY IMPLICIT
○ = STAGGERED I-I
△ = NODE-BY-NODE I-E
+ = ELEM-BY-ELEM I-E
× = DOF-BY-DOF I-E
◇ = FULLY EXPLICIT
2·10⁻²
10⁻¹
10⁰
CIRCULAR SAMPLING FREQ ωh

Figure 4

CONCLUSIONS

The material covered herein complements an earlier paper [1], which was devoted to the general categorization of partitioned integration procedures. The present paper expands on stability and accuracy as properties strongly related to the choice of extrapolation formula and computation path; these two aspects were only briefly commented upon in [1]. The information presented here may be used as an initial guide in method selection process. It whould be noted, however, that the selection of one partitioned procedure over another may be based on considerations other than those discussed here. For example, the availability of computational tools for treating certain subsystems of the overall problem (e.g., finite element structural analyzers, boundary-integral analyzers for infinite domains, etc.) may naturally dictate the use of certain partitions.

We have summarized in Table 6 general algorithmic characteristics of five partitioned solution procedures. From an unconditional stability viewpoint the implicit-implicit procedures (staggered and element-by-element partitions) would be preferred. This would be the case if the envisioned time stepsize is large compared to the shortest characteristic times of each subsystem.

Implicit-implicit partitions are desirable if subsystems display widely different response characteristics. They offer the advantage of computational simplicity for the explicitly-treated subsystems. From an applications viewpoint the element-by-element partition is natural for finite element discretizations, but can become cumbersome for extensively connected partitions (e.g., surface of volume-coupled finite element models). The node-by-node partition is estimated to require additional implementation effort, as "boundary nodes" must be appropriately labeled. It becomes attractive, however, when the number of boundary unknowns is considerable. The DOF-by-DOF

TABLE 6. ATTRIBUTES OF DIFFERENT PARTITIONED PROCEDURES

Partitioned Procedure	Boundary Rigid-Body Motions	Stability† (See Ref. 1)	Remarks
Element-by-Element I-E	Exact	$2/\omega_{HL}$	o Natural partition for coupled finite element programs o Inefficient for problems with many boundary unknowns
Node-by-Node I-E	Exact	$2/\omega_{BM}$	o Efficient for problems with many boundary unknowns o Modularization impaired because of implementation difficulties within implicit integrator
DOF-by-DOF I-E	Exact only for Path (CO')	$2/\omega_{DOF}$	o Allows degree-by-degree implicit (explicit) integration within each finite element
Staggered I-1	Inexact	Stable	o Accuracy loss may be a problem o Attractive for coupling finite element and boundary integral codes
Element-by-Element I-1	Exact	Stable	o No loss of accuracy due to partitioning o Natural partition for coupled finite element program

ω_{HL}, ω_{BM}, ω_{DOF} designate the maximum frequency of the explicitly partitioned domains.

partition, although less accurate than the previous ones, may be advantageous when the explicit-implicit partition is to occur within each element or node point of a finite element or finite difference model. An example would be the computational separation of translational and rotational degrees of freedom in lumped-mass finite element models.

We now summarize our main findings.

For a given integration formula, stability and accuracy of partitioned integration procedures are affected by the interaction of the computational path and selected extrapolator. The user is free to select partition-type, computational path, and extrapolator from many possible combinations. Such versatility is an important attribute of the present formualtion: implicit time-discretization, algebraic partitioning, and extrapolation. It is not shared by the "differential partitioning" formulation: partitioning at differential equation level, extrapolation, and time discretization, which was used in [2-6].

Possible distortion of rigid-body motions due to partitioning can be prevented for most partitions if the computation path (CO') in conjunction with a proper extrapolator are adopted. This is not the case when the differential partitioning approach is used except in the case of element-by-element and node-by-node partitions.

The primary error due to partitioning is manifested in frequency distortion for solution components adjacent to a partition boundary. Partition-caused numerical damping is of secondary importance. In particular, for integration formulas which possess no numerical damping, such as the trapezoidal and the central difference formulas, partitioning introduces no additional numerical damping if the extrapolator is judiciously selected.

ACKNOWLEDGMENTS

The authors wish to acknowledge support of this work by the Office of Naval Research under contract N00014-74-C-0355 and by the Lockheed Missiles & Space Company, Inc.'s Independent Research program.

REFERENCES

[1] Park, K. C., "Partitioned Transient Analysis Procedures for Coupled-Field Problems: Stability Analysis," to appear in Journal of Applied Mechanics.

[2] Belytschko, T., and R. Mullen, "Mesh Partitions of Explicit-Implicit Time Integration," Formulations and Computational Algorithms in Finite Element Analysis, ed. by J. Bathe, et al., MIT Press, 1977.

[3] Belytschko, T., and R. Mullen, "Stability of Explicit-Implicit Mesh Partitions in Time Integration," Int. J. Num. Meth. in Engr., Vol. 12, 1978, pp. 1575-1586.

[4] Park, K. C., C. A. Felippa, and J. A. DeRuntz, "Stabilization of Staggered Solution Procedures for Fluid-Structure Interaction Analysis," in Computational Methods for Fluid-Structure Interaction Problems, ed. by T. Belytschko and T. L. Geers, ASME Applied Mechanics Symposia Series, AMD-Vol. 26, 1977, pp. 94-124.

[5] Hughes, T. J. R., and W. K. Liu, "Implicit-Explicit Finite Elements in Transient Analysis: Stability Theory," J. Appl. Mech., Vol. 45, 1978, pp. 371-374.

[6] Hughes, T. J. R., and W. K. Liu, "Implicit-Explicit Finite Elements in Transient Analysis: Implementation and Numerical Examples," J. Appl. Mech., Vol. 45, 1978, pp. 375-378.

[7] Hughes, T. J. R., Private Communication, March 1979.

[8] Felippa, C. A. and K. C. Park, "Computational Aspects of Time Integration Procedures in Structural Dynamics: Implementation," J. Appl. Mech., Vol. 45, 1978, pp. 595-602.

[9] Irons, B. M. and A. Razzaque, "Experience with the Patch Test for Convergence of Finite Elements," Proc. Symp. on the Mathematical Foundation of the Finite Element Method with Applications to Partial Differential Operators, A. K. Aziz, ed., Academic Press, New York, 1972, pp. 557-587.

[10] von Neumann, J. and R. D. Richtmeyer, "A Method for the Numerical Calculations of Hydrodynamical Shocks," J. Appl. Phys., Vol. 21, 1950, pp. 232-257.

[11] Roache, P. J., "On Artificial Viscosity," J. Comp. Phys., Vol. 10, 1972, pp. 169-184.